



ACCEPTED MANUSCRIPT

This is an early electronic version of an as-received manuscript that has been accepted for publication in the Journal of the Serbian Chemical Society but has not yet been subjected to the editing process and publishing procedure applied by the JSCS Editorial Office.

Please cite this article as T. Vitomirov, B. Čobeljić, A. Pevec, D. Radanović, I. Novaković, M. Savić, K. Anđelković, M. Šumar-Ristović, *J. Serb. Chem. Soc.* (2023) <https://doi.org/10.2298/JSC230623044V>

This “raw” version of the manuscript is being provided to the authors and readers for their technical service. It must be stressed that the manuscript still has to be subjected to copyediting, typesetting, English grammar and syntax corrections, professional editing and authors’ review of the galley proof before it is published in its final form. Please note that during these publishing processes, many errors may emerge which could affect the final content of the manuscript and all legal disclaimers applied according to the policies of the Journal.



J. Serb. Chem. Soc. **00(0)**1-13 (2023)
JSCS-12258

Binuclear azide-bridged hydrazone Cu(II) complex: synthesis, characterization and evaluation of biological activity

TEODORA VITOMIROV¹, BOŽIDAR ČOBELJIĆ¹, ANDREJ PEVEC², DUŠANKA RADANOVIĆ³, IRENA NOVAKOVIĆ³, MILICA SAVIĆ³, KATARINA ANĐELKOVIĆ¹, MAJA ŠUMAR-RISTOVIĆ^{1*}

¹University of Belgrade – Faculty of Chemistry, Studentski trg 12–16, 11000 Belgrade, Serbia,

²Faculty of Chemistry and Chemical Technology, University of Ljubljana, Večna pot 113, 1000 Ljubljana, Slovenia, and ³University of Belgrade, Institute of Chemistry, Technology and Metallurgy, Department of Chemistry, Njegoševa 12, 11000 Belgrade, Serbia

(Received 23 June; Revised 27 June; Accepted 21 July 2023)

Abstract: The condensation product of 7-acetyl-6-azaindole and Girard's T reagent ((*E*)-2-(2-(1-(1H-pyrrolo[2,3-c]pyridin-7-yl)ethylidene)hydrazineyl)-*N,N,N*-trimethyl-2-oxoethan-1-aminium, **HL** ligand) was used as a ligand in the reaction with Cu(BF₄)₂·6H₂O and NaN₃. The reaction led to the formation of a binuclear Cu(II) complex containing two end-to-end (di- μ -_{1,3}-N₃) azide bridges, as well as two NNO-donor hydrazone ligands, forming an axially elongated square pyramidal geometry around each Cu(II) center. This end-to-end (di- μ -_{1,3}-N₃) azide bridge binding mode has not yet occurred in Cu(II) complexes containing the NNO-donor hydrazone ligands, which makes the structure of the complex even more interesting for further studies. The complex was characterized by elemental analysis, IR spectroscopy and X-ray crystallography, and it was found that it crystallizes in the triclinic space group P-1 with the asymmetric unit comprising one Cu(II) centre, zwitterionic ligand **L**, one azide (N₃⁻) ligand, and BF₄⁻ counter anion. Examination of antimicrobial activity of the complex shows higher antifungal and antibacterial activity towards tested Gram-positive bacteria in comparison to the hydrazone ligand, with the antifungal activity of the complex even being comparable to the activity of amphotericin B.

Keywords: Girard's T reagent; X-ray crystallography; antibacterial activity; antifungal activity.

*Corresponding authors E-mail: majas@chem.bg.ac.rs
<https://doi.org/10.2298/JSC230623044V>

INTRODUCTION

Azide-bridged binuclear copper(II) complexes have been the subject of considerable research in the field of coordination chemistry due to their interesting structural and magnetic properties.¹⁻³ These complexes consist of two copper(II) ions bridged by an azide group via either end-on (EO) or end-to-end (EE) coordination mode, forming single or double ligand bridges: $\mu_{1,1}$ -N₃ (EO) and $\mu_{1,3}$ -N₃ (EE).⁴

The azide group provides a unique building block for the construction of complex architectures and is a versatile bridging ligand that can adopt different coordination modes, such as mono-, bi- or tri-dentate,¹ depending on the nature of the metal ion and the reaction conditions. Furthermore, it also acts as a strong magnetic coupler facilitating ferromagnetic and antiferromagnetic coupling between metal ions within a binuclear complex.² On the other hand, the binuclear copper(II) complexes are known to exhibit either antiferromagnetic or ferromagnetic behavior, depending on the nature of the bridging ligand, the Cu–X–Cu angle and the geometry of the complex.^{3,5-9}

In recent years, there has been growing interest in the biological activity of binuclear copper(II) complexes due to their potential applications as anticancer^{10,11} and antibacterial¹²⁻¹⁴ agents. The ability of these complexes to catalyze the formation of reactive oxygen species (ROS) and to interact with DNA and proteins makes them attractive candidates for the development of new therapeutic agents. When discussing the azide-bridged binuclear Cu(II) complexes, several studies have reported the potential antibacterial activity of these complexes, all containing a tridentate NNO-donor hydrazone ligand, against various strains of bacteria.^{10,15,16} The mechanism of action is believed to be the disruption of the bacterial cell membrane due to the reduced polarity of the metal ion and increased lipophilicity of the formed complex, compared to lone metal ions and ligands.¹⁷

In addition to their biological applications, azide-bridged binuclear copper(II) complexes have also shown promising catalytic properties under sustainable and user-friendly conditions. These complexes have been reported to exhibit catalytic activity towards various reactions, including the N-arylation of imidazole and benzimidazole¹⁸ as well as the synthesis of 1,2,3-triazoles.¹⁹ The catalytic activity of these complexes is attributed to the redox properties of copper(II) ions and the Cu–N₃–Cu bridge, which can facilitate electron transfer processes.

In this study, we have synthesized and fully characterized a new binuclear copper(II) complex containing double end-to-end ($\text{di-}\mu_{1,3}$ -N₃) azide bridge, along with NNO-donor hydrazone ligands, and investigated its antibacterial and antifungal activities. The results of our study provide a detailed characterization of a binuclear copper(II) complex, as well as an overview of the potential of this complex as a new therapeutic agent.

EXPERIMENTAL

Materials and methods

All chemicals and solvents (reagent grade) were obtained from commercial suppliers (NaN₃ from Riedel-de Haën; all other chemicals from Sigma-Aldrich) and used without further purification. Elemental analyses (C, H, and N) were performed by standard micro-methods using the ELEMENTAR Vario ELIII C.H.N.S.O analyzer. IR spectra were recorded on a Nicolet 6700 FT-IR spectrometer using the ATR technique from 4000 – 400 cm⁻¹ (strong–s, medium–m, weak–w). NMR spectra were recorded with a Varian 400/54 PS spectrometer in deuterated dimethyl sulfoxide (DMSO-*d*₆).

Ligand synthesis

The ligand synthesis was carried out in two steps – the first step was obtaining 7-acetyl-6-azaindole using 7-bromo-6-azaindole as a starting compound. The reaction was performed by adding 0.75 mmol (18.2 mg) of Mg to 0.75 mmol (147 mg) of 7-bromo-6-azaindole in anhydrous diethyl ether and making a Grignard's reagent, which then reacted with equimolar amount (0.75 mmol, 58.9 mg) of acetyl chloride and a small amount (2 mol %) of FeCl₃ as a catalyst. This reaction was carried out at -60 °C using dry ice as a cooling bath.

The next step was to synthesize the condensation product of 7-acetyl-6-azaindole and Girard's T reagent, ((*E*)-2-(2-(1-(1H-pyrrolo[2,3-*c*]pyridin-7-yl)ethylidene)hydrazineyl)-*N,N,N*-trimethyl-2-oxoethan-1-aminium). The reaction was carried out by dissolving 0.5 mmol (80 mg) of 7-acetyl-6-azaindole in methanol and adding 0.5 mmol (83.8 mg) of Girard's T reagent to the reaction mixture, which was then refluxed for 3 hours. After cooling down to room temperature, the bright yellow precipitate was filtered and rinsed with ethanol. The reaction yield was 81 % (125.2 mg) and the ligand was then characterized by elemental analysis, IR and NMR spectroscopy. Labelling of C and H atoms described with NMR spectroscopy is presented in Fig. 1.

Elemental analysis for C₁₄H₂₀ClN₅O (%), Calculated: C 54.28, H 6.51, N 22.61. Found (%): C 54.68, H 7.09, N 22.13.

IR (ATR, cm⁻¹) selected peaks: 3377.4 (m), 3068.5 (m), 3019.4 (m), 2976.5 (m), 1703.4 (s), 1618.3 (w), 1571.8 (m), 1550.4 (m), 1491.2 (m), 1431.9 (m), 1398.4 (s), 1333.1 (m), 1280.2 (m), 1231.0 (m), 1164.0 (m), 1125.8 (m), 987.3 (m), 947.3 (m), 919.3 (m), 858.8 (w), 818.5 (m), 800.1 (m), 710.9 (m), 655.4 (m), 609.1 (w).

¹H NMR (400 MHz, DMSO-*d*₆), δ (ppm): 11.66 (s, 1H, N2-H), 11.50 (s, 1H, N4-H), 8.15 – 7.72 (4H, C1-H, C2-H, C4-H, C5-H), 4.91 (s, 2H, C11-H), 3.34 (t, 9H, C12-H), 2.32 (s, 3H, C9-H).

¹³C NMR (125 MHz, DMSO-*d*₆), δ (ppm): 167.24 (C10), 161.48 (C8), 156.29 – 120.21 (C1, C2, C3, C4, C5, C6, C7), 63.21 (C11), 53.74 (C12), 12.73 (C9).

Complex synthesis

The synthesis of the complex was performed by dissolving 0.25 mmol (77.3 mg) of ligand in 20 mL of methanol and then adding 0.25 mmol (86.3 mg) of Cu(BF₄)₂·6H₂O, previously dissolved in 5 mL of H₂O, and 1 mmol (65 mg) of NaN₃ directly into the reaction mixture. The mixture was refluxed for 2 hours, and after 10 days dark green monocrystals of complex were obtained and filtered from the solution. The reaction yield was 73 % (169.6 mg) and the complex was characterized by elemental analysis, IR spectroscopy and X-Ray crystallography.

Elemental analysis for C₂₈H₃₈B₂Cu₂F₈N₁₆O₂(%), Calculated: C 36.11, H 4.11, N 24.06. Found (%): C 35.74, H 4.25, N 24.58.

IR(ATR, cm^{-1}) selected peaks: 3350.3 (w), 3098.4 (w), 3044.3 (w), 2988.8 (w), 2063.4 (s), 1583.1 (s), 1557.8 (s), 1530.8 (s), 1501.3 (m), 1483.2 (s), 1441.4 (m), 1400.5 (m), 1347.7 (m), 1319.7 (m), 1296.1 (m), 1248.7 (m), 1185.3 (m), 1118.1 (m), 1034.8 (s), 997.2 (m), 972.1 (m), 926.3 (m), 910.6 (m), 815.7 (m), 733.2 (m), 655.2 (w).

X-ray structure determination

The crystal structure of compound $[\text{Cu}_2\text{L}_2(\mu_{1,3}\text{-N}_3)_2](\text{BF}_4)_2$ was determined by single-crystal X-ray diffraction methods. Crystallographic data and refinement details are given in Table I. Diffraction data were collected with Agilent SuperNova dual source diffractometer using an Atlas detector and equipped with mirror-monochromated $\text{MoK}\alpha$ radiation ($\lambda = 0.71073 \text{ \AA}$). The data were processed by using CrysAlis PRO.²⁰ The structure was solved using SIR-92²¹ and refined against F^2 on all data by full-matrix least-squares with SHELXL-2016.²² All non-hydrogen atoms were refined anisotropically. The nitrogen N2 bonded hydrogen atom was located in the difference map and refined with the distance restraints (DFIX) with $d(\text{N-H}) = 0.86 \text{ \AA}$ and with $U_{\text{iso}}(\text{H}) = 1.2U_{\text{eq}}(\text{N})$. All other hydrogen atoms were included in the model at geometrically calculated positions and refined using a riding model. The F4 fluorine atom in BF_4^- is disordered over two orientations and was refined with the use of PART instruction. The occupancy of F4a and F4b refined to the ratio of 55 and 45%, respectively. CCDC 2271001 contains the supplementary crystallographic data for this paper. These data can be obtained free of charge from The Cambridge Crystallographic Data Centre via www.ccdc.cam.ac.uk/data_request/cif.

TABLE I. Crystal data and structure refinement details for $[\text{Cu}_2\text{L}_2(\mu_{1,3}\text{-N}_3)_2](\text{BF}_4)_2$

formula	$\text{C}_{28}\text{H}_{38}\text{B}_2\text{Cu}_2\text{F}_8\text{N}_{16}\text{O}_2$
Fw (g mol^{-1})	931.44
crystal size (mm)	0.50×0.40×0.10
crystal color	green
crystal system	triclinic
space group	$P-1$
a (\AA)	7.8476(3)
b (\AA)	9.8765(6)
c (\AA)	13.2990(9)
α ($^\circ$)	110.341(6)
β ($^\circ$)	103.742(5)
γ ($^\circ$)	92.524(4)
V (\AA^3)	929.70(10)
Z	1
calcd density (g cm^{-3})	1.664
$F(000)$	474
no. of collected reflns	8891
no. of independent reflns	4259
R_{int}	0.0430
no. of reflns observed	3639
no. parameters	279
$R[I > 2\sigma(I)]^a$	0.0595
$wR_2(\text{all data})^b$	0.1815
Goof, S^c	1.051
$\Delta\rho_{\text{max}}/\Delta\rho_{\text{min}}$ ($\text{e}\text{\AA}^{-3}$)	+0.88/−0.80

$${}^a R = \sum |F_o| - |F_c| / \sum |F_o|, {}^b wR_2 = \{ \sum [w(F_o^2 - F_c^2)^2] / \sum [w(F_o^2)^2] \}^{1/2}$$

$${}^c S = \{ \sum [(F_o^2 - F_c^2)^2] / (n/p) \}^{1/2} \text{ where } n \text{ is the number of reflections and } p \text{ is the total number of parameters refined.}$$

Antimicrobial activity

In vitro antibacterial and antifungal activity was tested against four Gram-positive bacteria (*Bacillus subtilis* ATCC 6633, *Clostridium sporogenes* ATCC 19404, *Kocuria rhizophila* ATCC 9341, *Staphylococcus aureus* ATCC 6538), four Gram-negative bacteria (*Proteus hauseri* ATCC 13315, *Escherichia coli* ATCC 25922, *Pseudomonas aeruginosa* ATCC 9027, *Salmonella enterica* ATCC 13076), and three fungal strains (*Aspergillus brasiliensis* ATCC16404, *Candida albicans* ATCC 10231, *Saccharomyces cerevisiae* ATCC 9763), by the double dilution method in microtiter plates²³. Antibacterial activity was determined using Mueller Hinton broth, whereas antifungal activity was determined using Sabouraud dextrose broth. One hundred microliters of fresh Mueller Hinton or Sabouraud dextrose broth were added to each well of the plate. Then, 100 μ L of the compounds stock solution (10 mg/mL) prepared by dissolving compounds in DMSO was added. Each well was inoculated with 10 μ L (10^6 cells per mL) of bacterial cultures and 10 μ L (10^5 spores per mL) of fungal strains for antibacterial and antifungal determination, respectively. Bacterial strains were incubated at 37 $^\circ$ C for 24 h. Erythromycin was used as a positive control, while water served as a negative control. Fungal strains were incubated at 28 $^\circ$ C for 48 h. Amphotericin B was used as a positive control, while DMSO was used as a negative control. The bacterial growth was visualized by adding 20 μ L of 0.5% 2,3,5-triphenyltetrazolium chloride (TTC) aqueous solution.²⁴ The MIC was determined as the lowest concentration that resulted in inhibition of visible microbial growth.

The brine shrimp test

The brine shrimp test was performed against freshly hatched nauplii of *Artemia salina*.²⁵ The compounds were dissolved in DMSO and various amounts (0.01–1 mg) were added to artificial sea water containing 10–20 nauplii. After 24 h illumination at room temperature, the number of dead and surviving nauplii were counted and statistically analyzed. All samples were tested in triplicate. LC₅₀ was defined as concentration of compounds that caused the death of 50% of nauplii.

Assessment of radical-scavenging activity

Antioxidative activity of initial Cu(II) salt, appropriate ligand and the synthesized complex was determined using a DPPH (2,2-diphenyl-1-picrylhydrazyl) free radical scavenging assay. All tested compounds were dissolved in DMSO (stock concentrations were 10 mg/mL). For each tested compound, two rows of the 96-well microplate were used: one for measuring the absorbance of the compounds themselves and the other for antioxidant activity. 50 μ L of stock solutions of tested compounds were loaded into plate and double diluted by using multi-channel pipette. The rows used to measure the absorbance of the compounds were supplemented with 100 μ L of pure methanol, while the other rows were supplemented with 100 μ L of freshly prepared methanolic DPPH solution (6.58×10^{-5} M). In the control, 50 μ L pure DMSO was loaded. Final concentrations of the compounds ranged from (0.5 mg per well) to ($2.4 \cdot 10^{-4}$ mg per well). After 30 min of incubation at 37 $^\circ$ C in the dark, the absorption was measured at 517 nm. All measurements were done in triplicate. Free radical scavenging activity of compounds was measured using the equation:

$$\text{Activity} = 100 \times \frac{(A_{\text{sample}} - A_0)}{A_{\text{control}}} \quad (1)$$

where A_{control} is the absorbance of DPPH in the control probe, A_{sample} is the absorbance of DPPH in the samples, and A_0 is the absorbance of solutions of complexes 1 and 2 in DMSO, due to their intensive green colors. IC_{50} is defined as the concentration of antioxidant agent necessary to reduce the starting amount of DPPH by 50% and is calculated from the concentration-dependent free radical scavenging activity graph. Ascorbic acid was used as a control probe.

RESULTS AND DISCUSSION

The ligand synthesis was carried out in two steps, as presented in Fig. 1. After acetylation of 7-bromo-6-azaindole, the obtained 7-acetyl-6-azaindole reacted with Girard's T reagent in a molar ratio 1:1 and the ligand was formed. The complex was then obtained in the reaction of $\text{Cu}(\text{BF}_4)_2 \cdot 6\text{H}_2\text{O}$, ligand and NaN_3 in a molar ratio 1:1:4, as described in Fig. 2.

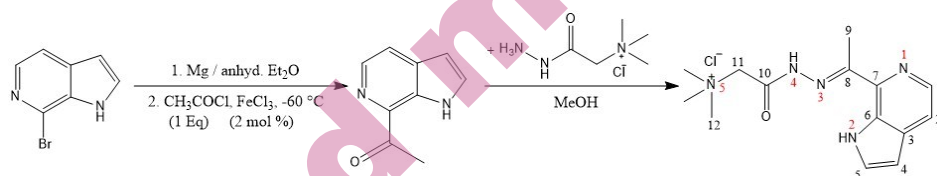


Fig. 1. Step by step ligand synthesis

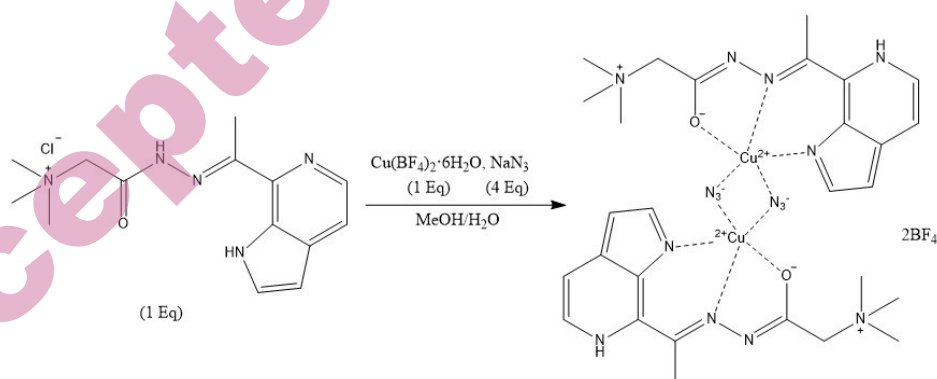


Fig. 2. Complex synthesis

IR spectra

IR spectroscopy confirmed the coordination of the ligand via the pyrrole nitrogen of 7-acetyl-6-azaindole ring. The stretching vibrational mode of the N–H group appears in the IR spectrum of the ligand as a wide band at 3377.4 cm^{-1} and disappears in the spectrum of the complex. The ligand spectrum also shows a very intense band at 1703.4 cm^{-1} , corresponding to the C=O stretching vibration of the carbonyl group. This peak does not appear in the spectrum of the complex, instead,

an intense peak appears at 1034.8 cm^{-1} , coming from the C–O stretching vibration. These all indicate the delocalization of the electron pair of the carbonyl group towards oxygen, which then favours the coordination of the ligand via the now negatively charged oxygen atom. The strong band appearing in the IR spectrum of the complex at 2063.4 cm^{-1} points out the presence of the N_3^- group in the complex structure.

X-ray crystal structure determination

Complex crystallizes in the triclinic space group $P\bar{1}$, with the asymmetric unit comprising one Cu(II) centre, zwitterionic ligand **L**, one azide (N_3^-) ligand, and BF_4^- counter anion. The crystal structure displays a centrosymmetric binuclear complex with the crystallographically independent Cu1 centre being coordinated to three donor atoms (N1, N3 and O1) of **L** and two N atoms (N6 and N8^a where $a = -x, -y, -z+1$) from two azide ligands which bridge two Cu(II) centres by adopting a double end-to-end ($\text{di-}\mu\text{-}_{1,3}\text{-N}_3$) coordination mode. The Cu1...Cu1^a separation is $4.8232(6)\text{ \AA}$. The molecular structure of the dimeric cationic moiety in the $[\text{Cu}_2\text{L}_2(\mu_{1,3}\text{-N}_3)_2](\text{BF}_4)_2$ complex and the atom-labelling scheme are shown in Fig. 3. Selected bond lengths and angles for the structure are given in Table S-I in the Supplementary material. The coordination polyhedron around Cu(II) is described as an axially elongated square pyramid with an index of trigonality (τ_5)²⁶ of 0.05 [$\tau_5 = (\beta - \alpha)/60$, where β and α are the two largest angles around the central atom]. The τ_5 is 0 for regular square based pyramidal geometry and 1.00 for regular trigonal bipyramidal geometry. The four in-plane bond distances are: Cu1–N1 $1.972(3)$, Cu1–N3 $1.975(3)$, Cu1–O1 $1.930(3)$ and Cu1–N6 $1.957(3)\text{ \AA}$, and the apical distance Cu1–N8^a (symmetry code $a = -x, -y, -z+1$) is $2.426(4)\text{ \AA}$. The azide anion bridges in an asymmetric (basal–apical) fashion so that the in-plane and axial Cu–N(N_3^-) bond distances are significantly different. The tridentate NNO coordination of **L** to Cu(II) ion generates one six-membered chelate ring (Cu–N–C–C–C–N) and one five-membered chelate ring (Cu–N–N–C–O) fused along the Cu1–N3 bond. The chelate rings are non-coplanar, as indicated by the dihedral angle of 3.8° . In this complex the Cu–N_{Ar} and Cu–N_{imine} bonds are comparable in length (Cu1–N1 $1.972(3)$ and Cu1–N3 $1.975(3)\text{ \AA}$, respectively). However, in Cu(II) complexes with two fused five-membered chelate rings generated by chelation of tridentate NNO donor hydrazone ligands the Cu–N_{Ar} bonds are longer than the Cu–N_{imine} bonds.^{27,28} Complex cations and BF_4^- anions generate a three-dimensional structure by means of intermolecular N–H...F, C–H...F and C–H...N hydrogen bonds given in Table S-II. In addition, the complex cations are connected by means of intermolecular $\pi\cdots\pi$ bonds extending in $[110]$ direction (Table S-III, Fig. S-1).

A search of the Cambridge Structural Database (CSD)²⁹ for the binuclear Cu(II)-azido complexes with hydrazone-based NNO-donor ligands revealed 12 crystal structures with double end-on ($\text{di-}\mu\text{-}_{1,1}\text{-N}_3$) coordination mode of bridging

azide anions. No crystal structure of binuclear Cu(II)-azido complex with tridentate NNO-donor hydrazone ligand having double end-to-end ($\text{di-}\mu\text{-1,3-N}_3$) coordination mode of bridging azides has been observed. The structure presented here is the first case. Details of CSD search are given in Table S-IV in the Supplementary material.

Crystallographic programs ORTEP-3 for Windows³⁰ and Mercury³¹ were used to prepare the drawings.

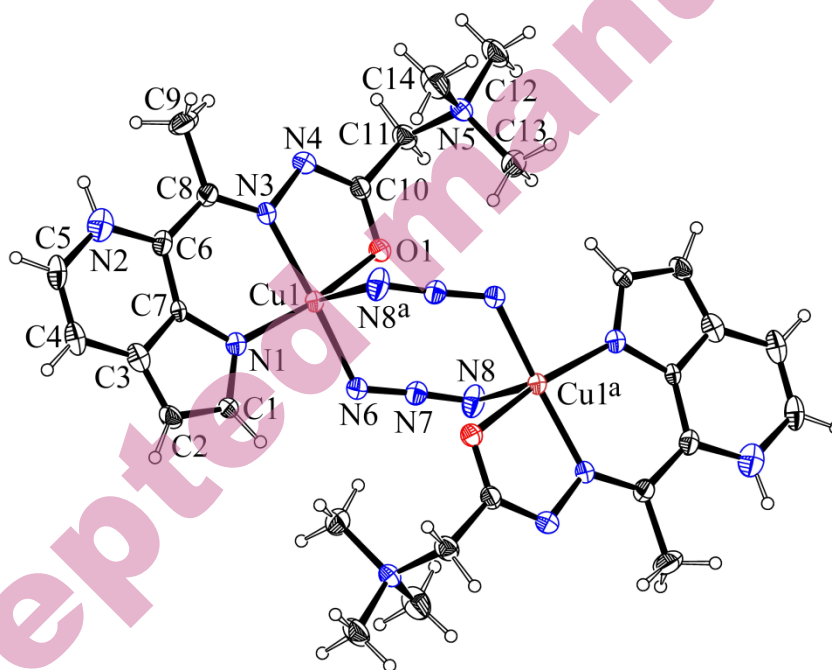


Fig. 3. ORTEP presentation of the complex cation $[\text{Cu}_2\text{L}_2(\mu_{1,3}\text{-N}_3)_2]^{2+}$ in $[\text{Cu}_2\text{L}_2(\mu_{1,3}\text{-N}_3)_2](\text{BF}_4)_2$. Thermal ellipsoids are drawn at the 30% probability level. The unlabeled part of the dimeric molecule is generated by symmetry operation $-x, -y, -z+1$.

Antimicrobial activity

Antimicrobial activity of the complex and the starting compounds ($\text{Cu}(\text{BF}_4)_2 \cdot 6\text{H}_2\text{O}$ and the ligand) was studied in DMSO solution by examining their minimum inhibitory concentration (MIC) on Gram-positive and Gram-negative bacteria and fungal strains. Erythromycin and amphotericin B were used as the standard drugs to compare the minimum inhibitory concentration values and the results are presented in Table II. Comparing the activities of the complex and the

ligand itself, the complex was shown to have higher antibacterial activity against all tested Gram-positive bacteria and half of the tested Gram-negative bacteria. The most significant difference between the antimicrobial activities of the complex and the ligand is the one against *S. aureus*, where the activity of the complex is 3 times higher than that of the ligand alone. The antifungal activities of the complex are significantly higher than those of the ligand, especially in the case of *S. cerevisiae*, where the antifungal activity of the complex is even comparable to the activity of amphotericin B.

TABLE II. Antimicrobial activity of the complex and the starting compounds (MIC values in mM)

Microorganism	Complex	Ligand	Cu(BF ₄) ₂ ·6H ₂ O	Standard ^{a,b}
<i>E. coli</i>	0.671	1.011	1.821	0.038
<i>P. aeruginosa</i>	0.671	1.011	3.642	0.076
<i>P. hauseri</i>	1.342	1.011	3.642	0.038
<i>S. enterica</i>	0.671	0.505	3.642	0.038
<i>S. aureus</i>	0.671	2.022	3.642	0.076
<i>C. sporogenes</i>	0.671	1.011	3.642	0.076
<i>K. rhizophila</i>	1.342	2.022	3.642	0.076
<i>B. subtilis</i>	0.671	1.011	3.642	0.076
<i>S. cerevisiae</i>	0.084	2.022	3.673	0.011
<i>C. albicans</i>	0.168	4.044	7.346	0.022
A. brasiliensis	0.356	4.044	3.673	0.044

^aStandard used for bacterial strains was erythromycin.

^bStandard used for fungal strains was amphotericin B.

The brine shrimp test

The brine shrimp lethality bioassay is an excellent predictive tool for the toxic potential of new bioactive compounds. The results of this test can be extrapolated to cell-line toxicity and anti-tumor activity.^{25,32} The results presented in Table III showed high toxicity of the ligand, compared to moderate toxicities of the complex and the Cu(II) salt. This moderate toxicity of the synthesized complex may indicate its potential as a new active drug.

TABLE III. Results of the brine shrimp test (LC₅₀, in mM) for the complex and the starting compounds

Compound	LC ₅₀ (mM)
Complex	0.613±0.051
Ligand	0.238±0.092
Cu(BF ₄) ₂ ·6H ₂ O	1.174±0.155
K ₂ Cr ₂ O ₇	0.077±0.016

Assessment of radical-scavenging activity

Assessment of radical-scavenging capacity was determined using a DPPH free radical scavenging assay and the results are presented in Table IV. According to

the obtained results, the basic salt and ligand did not possess DPPH radical scavenging capacity, whereas the complex showed moderate antioxidant activity.

TABLE IV. DPPH radical scavenging (IC_{50} , in mM) of starting compounds and the complex

Compound	IC_{50} (mM)
Complex	1.450±0.036
Ligand	7.834±0.126
Cu(BF ₄) ₂ ·6H ₂ O	>9.651
Ascorbic acid	0.079±0.003

CONCLUSION

In this paper we have thoroughly described the synthesis and characterization of a new binuclear azide-bridged Cu(II) complex containing NNO-donor hydrazone ligands obtained in a condensation reaction between 7-acetyl-6-azaindole and Girard's T reagent. The X-ray crystallographic analysis of the complex revealed a binuclear structure, in which two Cu(II) ions are bridged by two end-to-end (di- $\mu_{1,3}$ -N₃) azide ligands, while the hydrazone ligands coordinate to each Cu(II) center in a tridentate manner forming an axially elongated square pyramidal geometry around each metal ion. The complex crystallizes in the triclinic space group P-1. Detailed research of the Cambridge Structural Database revealed there are no crystal structures of binuclear Cu(II)-azido complexes with tridentate NNO-donor hydrazone ligands having double end-to-end (di- $\mu_{1,3}$ -N₃) coordination mode of bridging azides, making this complex structure unique and rather interesting. Antimicrobial activity of the complex was also examined, and it was shown that the complex exhibits higher antibacterial activity towards all tested Gram-positive bacteria than the ligand itself, while the antifungal activity of the complex towards all tested fungal strains was not only higher than that of the ligand, but also comparable to the activity of the standard drug. Results obtained in the evaluation of antimicrobial activity of the complex may indicate its potential as an antifungal agent.

Acknowledgment. This research has been financially supported by the Ministry of Science, Technological Development and Innovation of Republic of Serbia, contract numbers: 451-03-47/2023-01/200026, 451-03-47/2023-01/200168 and 451-03-47/2023-01/200288, as well as by the Science Fund of the Republic of Serbia, #7750288, Tailoring Molecular Magnets and Catalysts Based on Transition Metal Complexes – TMMagCat, and by the Slovenian Research Agency (ARRS), grant number P1-0175. We thank the EN-FIST Centre of Excellence, Ljubljana, Slovenia, for the use of the SuperNova diffractometer.

SUPPLEMENTARY MATERIAL

Supplementary Materials are available electronically from <https://www.shd-pub.org.rs/index.php/JSCS/article/view/12452>, or from the corresponding authors on request.

ИЗВОД

ДИНУКЛЕАРНИ ХИДРАЗОНСКИ КОМПЛЕКС Cu(II) СА АЗИДНИМ МОСТОМ: СИНТЕЗА, КАРАКТЕРИЗАЦИЈА И ЕВАЛУАЦИЈА БИОЛОШКЕ АКТИВНОСТИ

ТЕОДОРА ВИТОМИРОВ¹, БОЖИДАР ЧОБЕЉИЋ¹, АНДРЕЈ ПЕВЕЦ², ДУШАНКА РАДАНОВИЋ³, ИРЕНА НОВАКОВИЋ³, МИЛИЦА САВИЋ³, КАТАРИНА АНЂЕЛКОВИЋ¹, МАЈА ШУМАР-РИСТОВИЋ^{1*}

¹Универзитет у Београду – Хемијски факултет, Студентски бр 12–16, 11000 Београд, Србија,

²Факултет за хемију и хемијску технологију, Универзитет у Љубљани, Вена пош 113, 1000 Љубљана, Словенија, и ³Универзитет у Београду, Институт за хемију, технологију и металургију, Центар за хемију, Њевошева 12, 11000 Београд, Србија

Кондензациони производ 7-ацетил-6-азаиндола и Жираровог Т реагенса (лиганд HL) коришћен је као лиганд у реакцији са $\text{Cu}(\text{BF}_4)_2 \cdot 6\text{H}_2\text{O}$ и NaN_3 . Реакција је довела до формирања бинуклеарног Cu(II) комплекса који садржи два азидна моста у „end-to-end“ ($\text{di-}\mu\text{-}_{1,3}\text{-N}_3$) моду, као и два NNO-донорска хидразонска лиганда који заједно формирају аксијално издужену квадратно-пирамидалну геометрију око сваког централног металног јона. Овај „end-to-end“ ($\text{di-}\mu\text{-}_{1,3}\text{-N}_3$) азидни мост се до сада није појављивао у структурама бакар(II) комплекса који садрже NNO-донорске хидразонске лиганде, што чини структуру комплекса још интересантнијом за будућа испитивања. Овај комплекс је окарактерисан елементарном анализом, ИЦ спектроскопијом и рендгенском структурном анализом и пронађено је да кристалише у триклиничној просторној групи P-1 са асиметричном јединицом која се састоји из једног Cu(II) центра, цвтер-јонског лиганда (L), једног азидног лиганда (N_3^-) и BF_4^- контра-јона. Испитивање антимикуробне активности комплекса показало је вишу антифунгалну активност, као и вишу антибактеријску активност према Грам-позитивним бактеријама, у односу на сам хидразонски лиганд, док је антифунгална активност комплекса чак упоредива са активношћу амфотерицина Б који је коришћен као стандард.

(Примљено 23. јуна, ревидирано 27. јуна, прихваћено 21. јула 2023.)

REFERENCES

1. C. Adhikary, S. Koner, *Coord. Chem. Rev.* **254** (2010) 2933. (<https://doi.org/10.1016/j.ccr.2010.06.001>)
2. A. Escuer, G. Aromí, *Eur. J. Inorg. Chem.* **2006** (2006) 4721. (<https://doi.org/10.1002/ejic.200600552>)
3. K. Dankhoff, B. Weber, *CrystEngComm* **20** (2018) 818. (<https://doi.org/10.1039/C7CE02007D>)
4. M.R. Milenković, B. Čobeljić, K. Anđelković, I. Turel, *Eur. J. Inorg. Chem.* **2018** (2018) 838. (<https://doi.org/10.1002/ejic.201701387>)
5. P. Bhowmik, A. Bhattacharyya, K. Harms, S. Sproules, S. Chattopadhyay, *Polyhedron.* **85** (2015) 221. (<https://doi.org/10.1016/j.poly.2014.08.021>)
6. M. Das, B.K. Shaw, B.N. Ghosh, K. Rissanen, S.K. Saha, S. Chattopadhyay, *J. Coord. Chem.* **68** (2015) 1361. (<https://doi.org/10.1080/00958972.2015.1014350>)
7. P. Mukherjee, O. Sengupta, M.G.B. Drew, A. Ghosh, *Inorganica Chim. Acta.* **362** (2009) 3285. (<https://doi.org/10.1016/j.ica.2009.02.041>)
8. M.S. Ray, A. Ghosh, R. Bhattacharya, G. Mukhopadhyay, M.G.B. Drew, J. Ribas, *Dalton Trans.* (2004) 252. (<https://doi.org/10.1039/B311499F>)

9. S. Sen, S. Mitra, D.L. Hughes, G. Rosair, C. Desplanches, *Polyhedron*. **26** (2007) 1740. (<https://doi.org/10.1016/j.poly.2006.12.015>)
10. M.M. Fousiamol, M. Sithambaresan, K.K. Damodaran, M.R.P. Kurup, *Inorganica Chim. Acta*. **501** (2020) 119301. (<https://doi.org/10.1016/j.ica.2019.119301>)
11. T. Vitomirov, F. Dimiza, I.Z. Matic, T. Stanojković, A. Pirković, L. Živković, B. Spremo-Potparević, I. Novaković, K. Anđelković, M. Milčić, G. Psomas, M.Š. Ristović, *J. Inorg. Biochem.* **235** (2022) 111942. (<https://doi.org/10.1016/j.jinorgbio.2022.111942>)
12. T. Dimitrijević, I. Novaković, D. Radanović, S.B. Novaković, M. V. Rodić, K. Anđelković, M. Šumar-Ristović, *J. Coord. Chem.* **73** (2020) 702. (<https://doi.org/10.1080/00958972.2020.1740212>)
13. Sevda ER, H. Ünver, G. Dikmen, *Lett. Org. Chem.* **20** (2023) 376. (<https://doi.org/10.2174/1570178620666221202090558>)
14. D.Lj. Tomović, A.M. Bukonjić, V. V. Jevtić, Z.R. Ratković, J. V. Bogojeski, A. Đeković, I.D. Radojević, L.R. Čomić, S.B. Novaković, G.A. Bogdanović, S.R. Trifunović, G.P. Radić, S. Cupara, *Transit. Met. Chem.* **43** (2018) 137. (<https://doi.org/10.1007/s11243-018-0201-0>)
15. B. Shaabani, A.A. Khandar, F. Mahmoudi, M.A. Maestro, S.S. Balula, L. Cunha-Silva, *Polyhedron*. **57** (2013) 118. (<https://doi.org/10.1016/j.poly.2013.04.016>)
16. B. Shaabani, A.A. Khandar, H. Mobaiyen, N. Ramazani, S.S. Balula, L. Cunha-Silva, *Polyhedron*. **80** (2014) 166. (<https://doi.org/10.1016/j.poly.2014.03.033>)
17. P. Chakrabarti, *J. Mol. Biol.* **234** (1993) 463. (<https://doi.org/10.1006/jmbi.1993.1599>)
18. M.R. Milenković, A.T. Papastavrou, D. Radanović, A. Pevec, Z. Jagličić, M. Zlatar, M. Gruden, G.C. Vougioukalakis, I. Turel, K. Anđelković, B. Čobeljić, *Polyhedron*. **165** (2019) 22. (<https://doi.org/10.1016/j.poly.2019.03.001>)
19. R. Bikas, M.S. Krawczyk, T. Lis, *ChemistrySelect*. **5** (2020) 6759. (<https://doi.org/10.1002/slct.202001032>)
20. CrysAlis PRO, Oxford Diffraction Ltd., Yarnton, England, (n.d.).
21. A. Altomare, G. Cascarano, C. Giacovazzo, A. Guagliardi, *J. Appl. Crystallogr.* **26** (1993) 343. (<https://doi.org/10.1107/S0021889892010331>)
22. G.M. Sheldrick, *Acta Crystallogr. C Struct. Chem.* **71** (2015) 3. (<https://doi.org/10.1107/S2053229614024218>)
23. A. Rahman, M.I. Choudhary, W.J. Thomson, *Bioassay Techniques for Drug Development*, Harwood Academic Publishers, The Netherlands, 2001.
24. A. Sartoratto, A.L.M. Machado, C. Delarmelina, G.M. Figueira, M.C.T. Duarte, V.L.G. Rehder, *Braz. J. Microbiol.* **35** (2004) 275. (<https://doi.org/10.1590/S1517-83822004000300001>)
25. B. Meyer, N. Ferrigni, J. Putnam, L. Jacobsen, D. Nichols, J. McLaughlin, *Planta Med.* **45** (1982) 31. (<https://doi.org/10.1055/s-2007-971236>)
26. A.W. Addison, T.N. Rao, J. Reedijk, J. van Rijn, G.C. Verschoor, *J. Chem. Soc., Dalton Trans.* (1984) 1349. (<https://doi.org/10.1039/DT9840001349>)
27. T. Keškić, B. Čobeljić, M. Gruden, K. Anđelković, A. Pevec, I. Turel, D. Radanović, M. Zlatar, *Cryst Growth Des.* **19** (2019) 4810. (<https://doi.org/10.1021/acs.cgd.9b00760>)
28. M.R. Milenković, A.T. Papastavrou, D. Radanović, A. Pevec, Z. Jagličić, M. Zlatar, M. Gruden, G.C. Vougioukalakis, I. Turel, K. Anđelković, B. Čobeljić, *Polyhedron*. **165** (2019) 22. (<https://doi.org/10.1016/j.poly.2019.03.001>)

29. C.R. Groom, I.J. Bruno, M.P. Lightfoot, S.C. Ward, *Acta Crystallogr. B Struct. Sci. Cryst. Eng. Mater.* **72** (2016) 171. (<https://doi.org/10.1107/S2052520616003954>)
30. L.J. Farrugia, *J. Appl. Crystallogr.* **45** (2012) 849. (<https://doi.org/10.1107/S0021889812029111>)
31. C.F. Macrae, P.R. Edgington, P. McCabe, E. Pidcock, G.P. Shields, R. Taylor, M. Towler, J. van de Streek, *J. Appl. Crystallogr.* **39** (2006) 453. (<https://doi.org/10.1107/S002188980600731X>)
32. J.E. Anderson, C.M. Goetz, J.L. McLaughlin, M. Suffness, *Phytochem. Anal.* **2** (1991) 107. (<https://doi.org/10.1002/pca.2800020303>)

Accepted manuscript